CONCRETE LIBRARY OF JSCE NO.18, DECEMBER 1991

BEHAVIOUR AND PUNCHING STRENGTH OF RC SLABS DAMAGED BY CORROSION OF REINFORCEMENT

(Translation from Proceeding of JSCE, No.426/V-14, Feb. 1991)

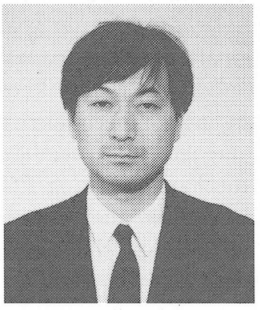

Yoshihiro TACHIBANA   Yasuo KAJIKAWA   Mitsunori KAWAMURA

SYNOPSIS

The failure mechanism and the punching strength of RC slabs damaged by corrosion of reinforcement are not only experimentally but also theoretically studied in order to obtain useful information for repair and maintenance. In the experiments, loading tests are conducted for RC slabs damaged with an accelerated galvanostatic corrosion method. It is found that the reduction in punching strength and the change of failuremechanism occurred in the damaged RC slabs. The modeling of failure mechanism of the damaged slabs is investigated by experimental and theoretical consideration using elastoplastic finite element analysis. From these consideration, it could be indicated that the punching strength of the damaged slabs is composed of the ultimate shear strength in compression zone under the loaded area and the bending strength of the main reinforcement with the bottom covers.

Y.Tachibana is a bridge engineer at Research Laboratory of Kawada Industries, Inc., Tokyo, Japan. He received his Master of Engineering Degree from Kanazawa University in 1984. His research interests include nonlinear analysis of concrete members and structures by the finite element method, mechanical behaviour and nondestructive testing method for damaged concrete members, durability of reinforced concrete decks for bridges, and composite structures. He is a member of JSCE, JCI and NDI.

Y.Kajikawa is a Professor of Civil Engineering at Kanazawa University, Kanazawa, Japan. He received his Doctor of Engineering Degree from Kyoto University in 1980. His research interests include nonlinear analysis of reinforced concrete members by the finite element method, and dynamic analysis of highway bridge. He was awarded a JSCE prize(Tanaka Prize) in 1976 for a series of studies on vibration serviceability of bridge. He is a member of JSCE and JCI.

M.Kawamura is a Professor of Civil Engineering at Kanazawa University, Kanazawa, Japan. He received his Doctor of Engineering Degree from Kyoto University in 1971. His research interests include alkari-aggregate reaction, effects of flyash on properties of concrete, and micro structure and fracture of concrete. He was awarded a JCI prize in 1984 and a CAJ prize in 1987 for a series of studies on alkari-silica reaction. He is a member of JSCE, JSMS, JCI, ACI and RILEM.

---

1. INTRODUCTION

In recent years, premature deterioration of the reinforced concrete structure that is typified by the damage by salt has been raising problems not only in Japan but also globally[1]. RC slabs of the road bridges could not be the exceptions and it is pointed out that deterioration of RC slabs could be increased in the future[2]~[3], because there are damages not only deiceing salt but also salty wind from the see and such salt is being accumulated year after year.

When RC slabs damaged by corrosion of reinforcement (hereinafter called "corroded RC slabs") are envisaged, evaluation of their safety should be discussed. As widely known, the ultimate strength depends upon the failure mechanism, namely the failure mechanism and the mechanical behaviour are supposed to be most important for damaged RC members. The authors once made an investigation on the change of the failure mechanism taking RC beams which had been damaged by galvanostatic corrosion[4]. From its results, they clarified that generation of internal stresses and cracks due to the expansion of corrosion products constitutes one of the causes of changing of failure mechanism, and suggested that corroded RC slabs are subject to the similar risk.

From these point of view, in this study, the failure mechanism and the method of estimation of the ultimate strength of corroded RC slab is not only experimentally but also theoretically studied. In the experiment, the loading tests were conducted for RC specimens damaged with an accelerated galvanostatic corrosion method and reduction in punching strength and changing mode of failure are observed. Based upon these experiment, the change of failure mechanism was estimated and the modeling of punching failure of corroded RC slabs was assumed. The experiment showed that the behaviour of corroded RC slabs corresponded to the assumed failure model, but it was difficult to obtain information to discuss the adequacy of assumed model only from the result of the experiment of this study. Therefore, it is attempted to apply the elasto-plastic finite element method as analytical study. In this paper, the result of these investigations was reported, discussion was made on a method to estimate the punching strength of the corroded RC slabs and information for making judgement on the safety of the corroded RC slabs was given.

2. EXPERIMENTS FOR CORRODED RC SLABS

2.1 Specimens

The RC slabs for loading tests are shown in Fig.1[5]. This was the full scale model of the RC slab of a road bridge with the thickness of the slab was 18cm and the double reinforcement were arranged in a similar manner of the actual structure. A pair of the opposite side of the slab were simply supported and the other pair were free. Connection with the steel girders that supported the slab was made with the slab anchors providing the hunches of 3cm. The reinforcing bars used in this experiment were deformed bars, those of D19 were used for main reinforcement and D16 for distribution reinforcement. The mix proportion of concrete was shown in Table 1, its compressive strength was 24.0MPa and modulus of elasticity was 2.75×10^5MPa. The yielding strength of the steel bars was 3,610MPa. 4 pieces of specimens were built and used in the loading tests.

2.2 Galvanostatic Corrosion of Reinforcement

As the method of accelerated corrosion, the galvanostatic method was adopted[4]. This method causes uniform corrosion of whole body of reinforcement, and it is possible to control the degree of corrosion by integration of electric current. In this experiment, the specimens which were corroded under the condition of electric current density 0.4mA/cm^2 for 19 days were used. This integration of electric current corresponded to that of the corroded RC beam to which the authors had applied the loading tests and the reduction of load carrying capacity had been recognized in the previous study[4]. The percentage of weight loss at that time was about 5% in terms of the difference in weight measured before and after removal of rust with the solution of citric 2 ammonium. Examples of the cracks generated in the bottom and side surface of the slab caused by expansion of corrosion products are shown in Fig.2,3.

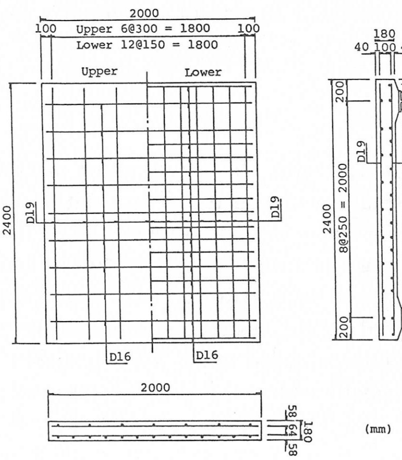

Fig.1 RC Slab Specimen.

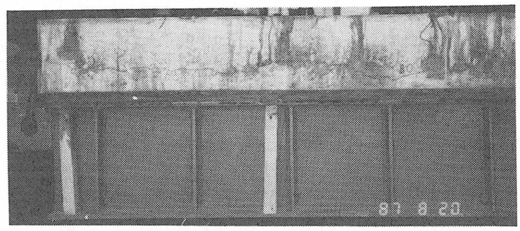

Fig.2 Cracks after Galvanostatic Corrosion at Side Surface.

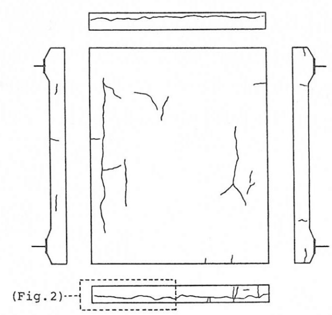

Fig.3 Cracks after Galvanostatic Corrosion.

Table 1 Mix Proporation of Concrete.

Slump (cm)	Maximum Size of Coares Aggregate (mm)	Air Content (%)	Water Cement Ratio (%)	Sand Percentage (%)
8.0	25	4.0	46.5	41.4

In the case of the RC beam reported in the literature[4], cracks were generated along the axes of steel bars on the bottom surface of the beam, but they did not appear so conspicuously in these slabs. In contrast with the observed conditions, it was confirmed from the inspection made after loading test that the reinforcement was corroded as a whole shown in Fig.4, and

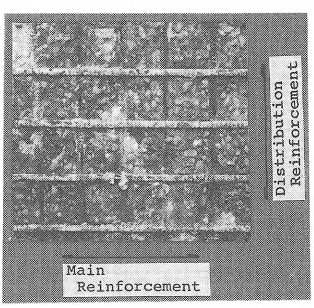

Fig.4 State of Rust Sludge.

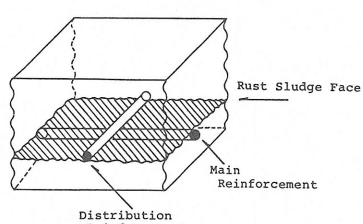

Fig.5 Rust Sludge Face.

that rust sludge was spread along the horizontal plane shown in Fig.5. This horizontal plane was generated between the main reinforcement and the distribution reinforcement. In this specimen, it grew forming a horizontal cleavage plane.

With regard to the generation of cracks in RC slabs of the road bridges damaged by corrosion of reinforcement, it is also reported in U.S.A. that partial cleavage surface are generated within the slabs horizontally as examples of damages[6]. In this case of natural corrosion, occurrence of local damages or unevenness is inevitable, and galvanostatic corrosion and natural one do not always correspond each other in their consequences. However, when the fundamental investigation on the mechanical behaviour is aimed at, it is supposed to be made minimizing uncertain condition factors such as unevenness and it could adopt the aforementioned RC slab specimens whose reinforcement had been uniformly corroded as one of the models for investigating their mechanical behaviour.

2.3 Loading Tests

The loading test for the RC slab specimens were conducted with the servo-pulser of the capacity of 60tf and the load was applied statically by displacement control. The position of the loading plate shown in Fig.6(a) was at the center of the slabs and the dimensions of the loading plate were determined to be 20 × 50 cm, envisaging the wheel load provided in the specifications for highway bridge. The position of strain gauges were attached at the bottom reinforcement are shown in Fig.7. Out of 4 specimens used in the tests, 2 specimens were damaged by galvanostatic corrosion and 2 specimens were non-corroded ones. Two specimens out of them (one each of corroded and non-corroded specimen) were subjected to the cyclic loading in accordance of the scheme as shown in Fig.6(b) and Table 2, and after that static loading up to 60tf was applied.

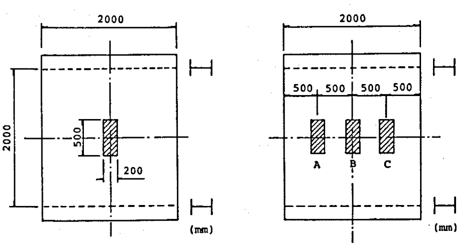

(a) Loading Point. (b) Cyclic Loading.

Fig.6 Loading Tests.

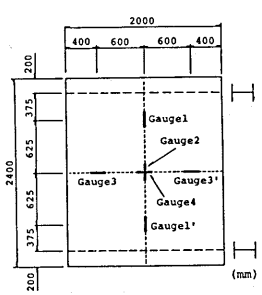

Fig.7 Strain Gauges at Reinforcement.

Table 2 Cyclic Loading.

Loading Step	Cyclic Loading		
	Point	Amplitude	No. of cycle
1	B	0 - 24 tonf	1
2	C	0 - 24 tonf	1
3	A	0 - 24 tonf	1
4	B	0 - 24 tonf	1
5	C	0 - 24 tonf	1
6	A	0 - 24 tonf	1
7	B	0 - 24 tonf	1
8	B	0 - 12 tonf	10,000
9	C	0 - 12 tonf	10,000
10	A	0 - 12 tonf	10,000
11	B	0 - 16 tonf	10,000
12	B	0 - 24 tonf	10,000
13	C	0 - 24 tonf	10,000
14	A	0 - 24 tonf	10,000
15	B	0 - 36 tonf	10,000

As a part of the result of the loading tests, the relation between the load and the displacement at the center of RC slab to which the cyclic load has not been applied is shown in Fig.8, the status of cracks generated after the loading test in Fig.9, and the relation between the load and the strain of the reinforcement in Fig.10,11.

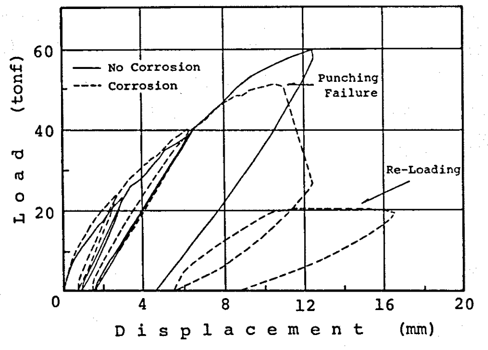

Fig.8 Load - Displacement Relation.

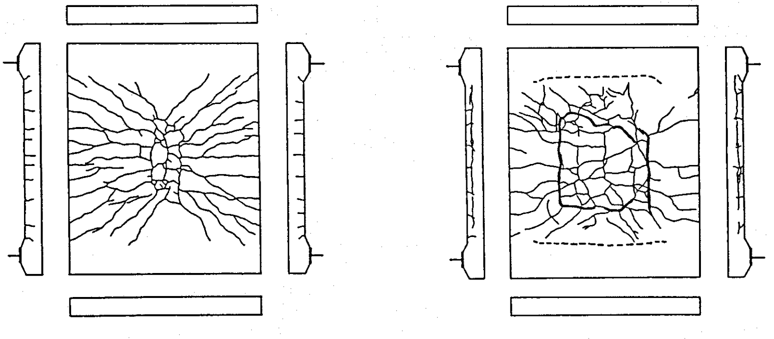

(a) No Corrosion.

(b) Corrosion (Failure).

Fig.9 Crack Pattern.

Judging from the diagrams of Fig.8, the load-displacement curves of both specimens almost coincide until the load reaches about 40tf, however, in the non-corroded RC slab, failure did not take place even when loaded up to 60tf which was the maximum capacity of the testing machine. In the corroded slab, its flexural rigidity came down after the load exceeded 45tf and punching failure occurred at 51.5tf. This punching failure presented a subsidence just under the loading plate on the top surface and the pattern of cracks on the bottom surface was shown in Fig.9(b). In this mode of failure, splitting fracture at the bottom surface, which was generally reported as the shape of punching failure of RC slab of the road bridge[7], was not observed. By the way, as the loading was being done by the displacement control method, reloading after punching failure was possible and the specimen held the strength of 20.1tf when reloaded. In this reloading, the width of the cracks indicated with thick lines shown in Fig.9(b) grew faster than other cracks, the shape of the deflected bottom surface was observed that the knuckles were generated at these cracked parts. Then, when the displacement was further increased after the maximum load, generation of cracks that causes peeling off was observed at the position as shown with dotted line in Fig.9(b).

The RC slab specimens to which cyclic loading was applied displayed a similar behaviour. In the case of non-corroded RC slab, no failure took place by loading up to the maximum load 60tf, and in the case of corroded RC slab, punching failure occurred at 56.5tf showing similar mode of failure and the maximum load was 18.3tf when reloaded.

It was found that there were differences between the behaviour of the strain shown in Fig.10 and Fig.11, especially in Gauge 1 of the main reinforcement, its behaviour was supposed to be related with the failure mechanism. As the factors that affected these behaviour, such as the changes of properties of the friction, cohesion and mechanical engagement between concrete and reinforcement, existence of cracks or existence of residual strain in the reinforcement due to expansion of corrosion products[5], were considered.

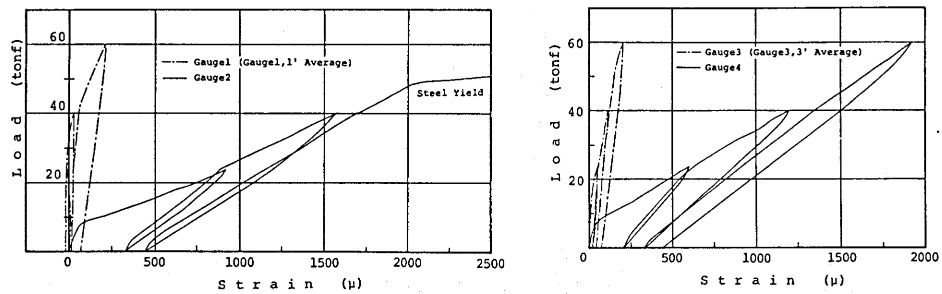

(a) Main Reinforcement. (b) Distribution Reinforcement.

Fig.10 Load - Strain Relation (No Corrosion).

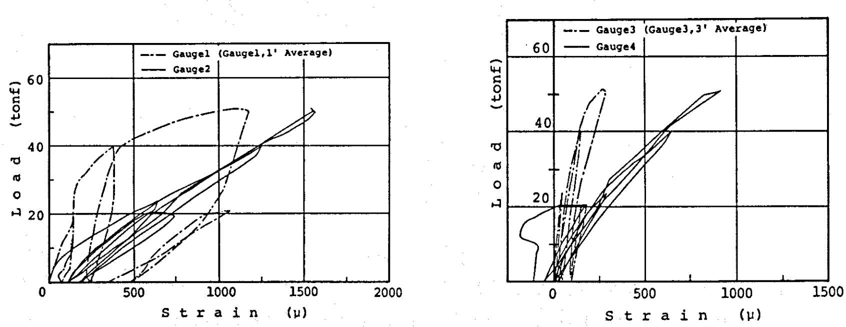

(a) Main Reinforcement. (b) Distribution Reinforcement.

Fig.11 Load - Strain Relation (Corrosion).

2.4 Subjects to be Investigated

As the result of loading tests, reduction in punching strength of corroded RC slabs were confirmed. Judging from the mode of failure observed in the experiment, this reduction in punching strength was presumed to be caused by the difference of failure mechanism between the non-corroded RC slab and corroded one and it was supposed to have some connection to the status of the damages by galvanostatic corrosion. As mentioned previously, in order to evaluate the safety of the corroded RC slabs, it is essential to estimate their strength. For that purpose, the failure mechanism of corroded RC slabs must be made clear. Accordingly, in the following sections, investigations on the modeling of failure of corroded RC slabs that could explain the result of experiment presented above and the method of estimating the strength are going to be made.

3. MODELING OF FAILURE OF CORRODED RC SLABS

In this section, discussion is made on the punching failure of a sound RC slab and an investigation is made as well on the modeling of the failure of the corroded RC slab that changes as shown by the conditions of damage mentioned in the above.

3.1 Punching Failure of Sound RC Slabs

When the punching failure of RC slabs takes place, its failure mechanism is complicated because of the conditions that the structure of the slab itself is statically indeterminate structure of a high order, that its behaviour is affected by the condition of loading, condition of supporting and constraint and that its failure is the 3-dimensional phenomena[8],[9]. With regard to the ultimate strength, it has been reported that it is influenced many facters such as the strength of concrete, shape and dimensions of the loading plate, thickness of the slab, arrangement of the reinforcement and so forth, as the results of studies in the past[7]~[12]. These factors vary widely depending upon the use of the slab and if the slabs are dealt with as the object in general including the slabs for road bridge, the failure mechanism that could explain reasonably including all these conditions has not yet been fully clarified at present because of its complexity. The method of calculation for the ultimate strength therefore depends mostly upon the empirical formulae, among which Kakuta's formula[11] is well known in Japan and in the specifications for concrete empirical formulas are also adopted[13].

On the other hand, when the limited structure, namely the RC slab for road bridge is chosen as the object, it has been reported that the punching strength could be estimated with fairly accuracy by Matsui's formula as shown in the following[14]. This formula is based upon the failure mechanism and as shown in Fig.12, it is derived under the assumption that the shearing fracture just under the loading plate and the splitting fracture of the cover concrete due to the dowel action of the reinforcement.

$$P = \tau_{s,max}(2(a+2X_m)X_d + 2(b+2X_d)X_m) + \sigma_{t,max}(2(a+2d_m)C_d + 2(b+2d_d+4C_d)C_m) \quad (1)$$

where,

a,b: Length of the sides along the directions of the main reinforcement and the distribution reinforcement respectivity (cm)

X_m,X_d: Distances of the neutral axes of the cross sectionnormal to the main reinforcement and the distribution reinforcement respectively disregarding the cross section of concrete in the tension side (cm)

d_m,d_d: Effective hights to the main and distribution reinforcement respectively (cm)

C_m,C_d: Distances between the center of the main reinforcement on the tension side and the distribution reinforcement on the tension side to the bottom surface of concrete (cm)

$\tau_{s,max}$: Maximum shearing stress of concrete (kgf/cm^2)

$\sigma_{t,max}$: Maximum tensile stress of concrete (kgf/cm^2)

With regard to $\tau_{s,max}$ and $\sigma_{t,max}$ referred here, it was mentioned in the literature[7] that they were related to the compressive strength σ_{ck} of concrete and Ito's formula and Okamura's formula as shown in the following were effective.

$$\tau_{s,max} = 0.252\sigma_{ck} - 0.000246\sigma_{ck}^2 (kgf/cm^2) \quad (2)$$

$$\sigma_{t,max} = 0.583\sigma_{ck}^{2/3} (kgf/cm^2) \quad (3)$$

Since the object of this study is the RC slab of the load bridge, the failure mechanism as shown in Fig.12 and the formula(1) are supposed to be applied. Further investigation is decided to be made based upon this failure mechanism. According to the result of caluculation made by the formula(1), the non-corroded RC slab used in the loading test gave the strength of 71.7tf and failure did not take place at the maximum load of 60tf which endorsed the result of the experiment.

3.2 Modeling of Punching Failure of the Corroded RC Slab

In the formula(1), the 1st term represents the shearing fracture just under the loading plate and the 2nd term represents the splitting fracture of of the cover concrete due to the dowel action of the reinforcement respectively. In the corroded RC slab, if judged from the existence of cracks due to expansion of corrosion products forming a horizontal cleavage plane as previously mentioned and difference in the mode of failure, it is readily presumed that the influence of the dowel action on the punching strength is smaller than that in the non-corroded RC slab. As shown in Fig.13(a), in the sound RC slab the tensile stress is introduced into concrete by this dowel action and cracks are generated. However, since, in the case of corroded RC slab, there exists the cleavage forming a horizontal plane which was generated by the swelling of corrosion products along the same direction as that of these splitting cracks as shown in Fig.5, the dowel action itself become almost ineffective. In other words, as illustrated in Fig.13(b), it is clear that the cover including the reinforcement takes a behaviour to be peeled off by the vertical force V which is transmitted to the reinforcement by way of the diagonal cracks, and this is supposed to be the reason for the fact that no clear of trace of splitting fracture due to the dowel action appeared on the bottom surface of the slab in the experiment.

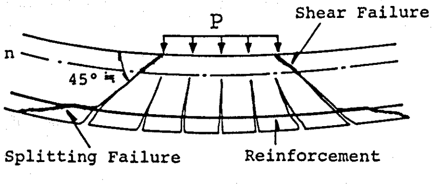

Fig.12 Modeling of Punching Failure of RC Slabs.

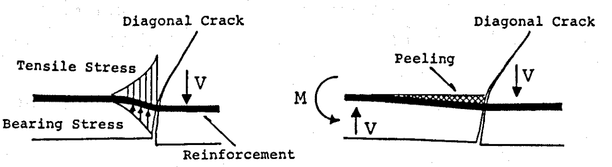

(a) No Corrosion (Dowel Action). (b) Corrosion.

Fig.13 Transmission of Shear Force at Diagonal Crack.

In consideration of these condition, a model as illustrated in Fig.14 is assumed as the modeling of punching failure for corroded RC slabs. In this model, in addition to the shearing fracture just under the loading plate similar to the 1st term which has been represented by the formula(1), the maximum vertical force V_{max} which can be transmitted through the diagonal cracks, as an item that contribute to the punching strength, and it is assumed that the punching strength of the corroded RC slab is determined by these two items. Here, the dowel action of the reinforcement on the compression side is disregarded. This maximum vertical force V_{max} as shown in Fig.14 is defined to be the force which is equilibrated with M_u, the resisting moment against yielding failure of the reinforcement at the cross section which is composed of the cover including the reinforcement on the tension side.

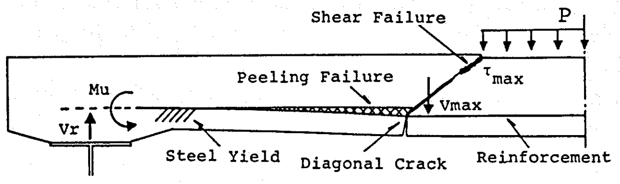

Fig.14 Modeling of Punching Failure of Corroded RC Slabs.

By the way, the weight loss of reinforcement is considered among the conditions of damage. But, since the strength of the slab is decided by punching shear failure, the amount of the weight loss of 5% in this experiment could influence little on the punching strength.

3.3 Correspondence to the Behaviour during the Loading Tests

In this paragraph, some examination on the failure model as assumed in Fig.14 and its behaviour in the loading tests is going to be made.

If, in the failure model illustrated in Fig.14, the vertical force V_{max} that is transmitted by way of the diagonal cracks is to be determined by the resisting moment M_u against yielding failure of the reinforcement, it could be expected that the transmitting mechanism of forces as shown in Fig.13(b) survives even after the punching failure, and the strength holds when reloaded and the vertical force V_{max} would coincide. Now, under the assumption that the share of contribution to the punching strength against the shearing fracture just under the loading plate follows the 1st term of the formula (1), the values of the punching strength evaluated by adding the values calculated by this 1st term to the strength holds when reloaded, are shown in Table 3. It is found that these values almost coincide with the strength of the corroded RC slabs. Accordingly, if the failure model assumed in Fig.14, is followed, it would be confirmed that V_{max} coincides with the strength holes when reloaded.

Table 3 Ultimate Strength.

Specimen	First Term in eq.(1) A	Ultimate Sterngth in Re - Loading B	A+B	Punching Strength of RC Slabs in Experiment
Without Cyclic Loading	38.1 tonf	20.1 tonf	58.2 tonf	51.5 tonf
With Cyclic Loading	38.1 tonf	18.3 tonf	56.4 tonf	56.5 tonf

On the other hand, in the load-displacement relation when reloaded, which was shown in Fig.8 as the result of experiment, its ductile behaviour closely resembles that of RC beams applied bending moment, thus it is presumed probable that yielding of the reinforcement has taken place. With regard to the strain in the reinforcement, the reading Gauge 1 which was guess to be related with the failure mechanism indicated that the tensile force was generated when reloaded as shown in Fig.11(a). This fact is supposed to correspond to the behaviour of the cover including main reinforcement as if it is peeling off.

By the way, It must be noted that the failure model assumed in Fig.14 holds good under condition that the yielding of the reinforcement and the shearing fracture are generated simultaneously. In order to satisfy this condition, the deflection that has been generated just before the punching failure should be larger than that which is required for generating the yielding of the reinforcement in the equilibrium system shown in Fig.14. If it is assumed that the plastic flow where shear fracture took place does not contribute to the flexural rigidity stiffness in the equilibrium system in Fig.14, this amount of deflection is supposed to be evaluated by the portion of the elastic deflection when reloaded in accordance with the result of the experiment as shown in Fig.8, which similar reasoning to that mentioned in the above. If comparison is made based on this reasoning between the amount of deflection at punching failure of the slab and the elastic portion of the deflection when reloaded with reference to the test result as shown in Fig.8, the former is greater than the latter. Therefore, the result of the experiment would be regarded to indicate that yielding of the reinforcement and the shearing fracture could occur simultaneously in the model assumed in Fig.14.

As discussed in the above, the necessary conditions for this failure model were given by the result of experiment described in the previous section. However, the result of experiment obtained in this study only by itself could not provide the conditions in full to discuss the adequacy of this model. Thus,the analytical investigation by using the finite element method is going to be made in the following section.

4. FAILURE MODEL AND PUNCHING STRENGTH

In the previous section, if a failure model shown in Fig.14 in which the vertical force V_{max} was determined by resisting moment due to yielding of the reinforcement was assumed, this vertical force V_{max} which was transmitted by way of the diagonal cracks could be evaluated with the ultimate strength when reloaded. Inversely, if the behaviour when reloaded is traced by means of the analysis and it is proved that the ultimate strength when reloaded is determined by the resisting moment due to yielding of the reinforcement, the sufficient conditions could be satisfied, and it could be made one of the method to verify the adequacy of this failure model. In this section taking the view mentioned above, the adequacy of this model by the finite element method and the method of estimation of the ultimate strength of the corroded RC slab, are investigated.

4.1 Finite Elements

The behaviour was supposed to take place in the part of the cover including the main reinforcement when reloaded, analytical modeling was made taking the hatched portion in Fig.15 as the object of analysis.

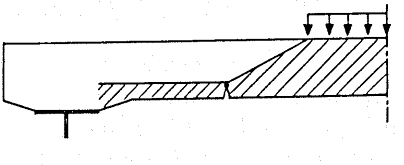

Fig.15 Subject to the Analysis.

The analysis is made on the 1/4 model considering the symmetric conditions, and the plate bending element was used for the finite element. In Fig.16, the thickness of the plate bending elements for calculating the geometrical moments of inertia are shown. The condition at the boundaries were assumed to be perfectly fixed along the steel girders. And in order to model the condition under which the vertical forces only were transmitted to the reinforcement by way of the diagonal cracks, the spring elements to the vertical direction that connect the nodal points are inserted. These nodal points were chosen along the thick line drawn in Fig.9(b), in other words, the spring elements were placed at the positions corresponding to the positions of the diagonal cracks and as their spring constant, 1.0×10^{10} kgf/cm was used which was equivalent to perfect adhesion. By the way, division of the elements was determined by taking into the position of the loading plate, the pitch of the main reinforcement and the position of the spring elements.

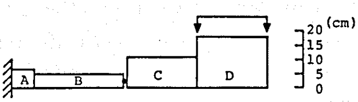

(a) Thickness of Elements.

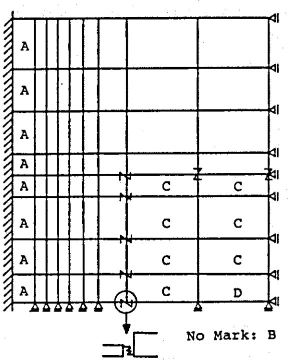

(b) Elements.

Fig.16 FEM Analysis.

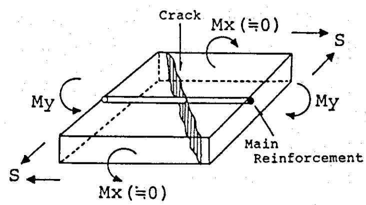

Fig.17 Stiffness for the A,B Elements.

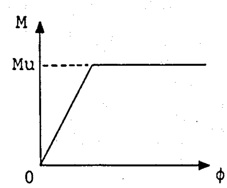

Fig.18 Proposed Relation between M and ϕ.

4.2 Characteristics of the Elements

In this analysis, the plate bending elements were dealt with as reinforced concrete plate and expressed, the flexural rigidity of these elements were expressed with consideration of the stress-strain relation as explained hereunder.

a) Elastic Region As the characteristics of the plate element, C and D elements illustrated in Fig.16 were assumed to be isotropic and elastic bodies. On the other hand, with respect to A and B elements, whose cross section were made in the cover, their anisotropic condition must be presented, because cracks were generated within the element shown in Fig.17 and what could bear the tensile force was the main reinforcement only. For that purpose, the formula (4) was assumed as the stress-strain relation along the direction within the plane. Where E and G were elastic modulus and shearing modulus of concrete respectively, and α and β were the coefficients that took the values of 0~1.

$$\begin{Bmatrix} \sigma_x \\ \sigma_y \\ \tau_{xy} \end{Bmatrix} = \begin{bmatrix} \alpha E & 0 & 0 \\ 0 & 0 & 0 \\ 0 & 0 & \beta G \end{bmatrix} \begin{Bmatrix} \varepsilon_x \\ \varepsilon_y \\ \gamma_{xy} \end{Bmatrix} \quad (4)$$

As the anisotropic condition, the mono-axial condition were considered in the formula (4) and it was assumed that the stress was transmitted along the main reinforcement only as the axial stress component. And as for the shearing stress component, it was assumed to the transmitted through the interlocking effect along the cracked surface. With regard to the flexural rigidity along the direction of the main reinforcement, the coefficient α was introduced, envisaging that it took a certain value between the flexural rigidity with the cross section working in full and with neglected sectional area on the tension side. In the analysis, the flexural rigidity with full cross section working effectively is determined at α =1.0 and in case the flexural rigidity when concrete on the tension side is disregarded is going to be represented, it can be made by setting the value α as its ratio to the flexural rigidity with full cross section working effectively. For the element B which was anticipated to become dominant in the elasto-plastic analysis, the flexural rigidity with disregarded concrete on the tension side was to be represented with the value of α =0.78. On the other hand, with regard to the shearing rigidity, the transmissibility of the shearing stress varies widely depending upon the condition of cracks, and referring to the literature[15] it was assumed to vary over the range of β =0.1~1.0. Accordingly, in the analysis, the case of α =1.0, β =1.0 and that of α =0.78, β =0.1 were considered.

b) Plastic Region In this analysis, the elasto-plastic relation of the plate element was given in the form of the moment-curvature relation. As the mode of failure of the element, yielding of the reinforcement and collapse of concrete were considered. However, no trace of collapse was observed even when the ultimate strength was reached in the experiment. Therefore in this analysis, only yielding of the reinforcement was considered in the analysis. The moment-curvature relation along the direction of the main reinforcement in the analysis was assumed as shown in Fig.18, and when the resisting moment of the element was reached, the flexural rigidity along the direction of the main reinforcement was made zero or α =0. At this time, β was made zero, too. The calculation of the resisting moment of each element was assumed to be made by the formula (5) in accordance with the specifications for highway bridges.

$$M_u = A_s \sigma_{sy} (d - A_s \sigma_{sy} / 1.7 \sigma_{ck}) \quad (5)$$

where,

M_u: Fracture resisting moment per unit breadth (kgf·cm/cm)
σ_{ck}: Compressive strength of concrete (kgf/cm^2)
σ_{sy}: Yielding strength of the reinforcement (kgf/cm^2)
A_s: Sectional area of the reinforcement per unit breadth (cm^2/cm)
d : Effective height (cm)

4.3 Method of Analysis

The analysis was conducted by the load increment analysis and rmim method[16] in which the load increment was controlled so that the element yield one by one. In this method, at every step, a unit load was applied as the testing load, and for every element, the exact amount of increment of load necessary for yielding the element was obtained in advance and the minimum value among them is adopted as the increment of load. This analysis was continued until the rigidity reaches null.

4.4 Result of the Analysis

As the result of the analysis, the relation of load-displacement at the center of slab was shown in Fig.19 and the element whose reinforcement has yielded in Fig.20.

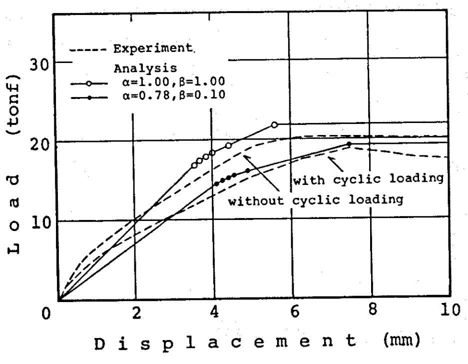

Fig.19 Comparison between Experiment and Analysis.

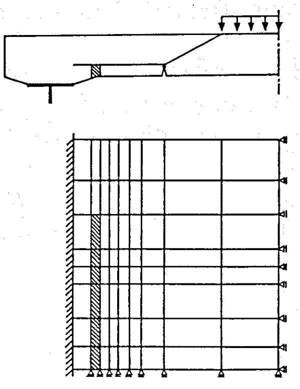

Fig.20 Yielding Elements.

In Fig.19, in addition to the result of analysis, that of the RC slabs as the result of experiment, one of them was given cyclic loading and the other was not. Regarding the ultimate strength the specimens held when reloaded, the values by analysis could be said to coincide almost with those by experiment. According to the result of analysis, if the case of $\alpha=1.0$, $\beta=1.0$ and the case of $\alpha=0.78$, $\beta=0.1$ were compared, the ultimate strength of the latter was smaller than that of the former by about 15% and the rigidity of the latter was smaller. In the experiment, it was anticipated the values of α and β of the RC slab with cyclic loading became smaller than those of the RC slab without it. The result of the analysis that as the values of the coefficients α and β got smaller, the rigidity and the ultimate strength tended to decrease looks to show a similar trend to that of the result of the experiment.

The elements shown with hatching in Fig.20 were the yielded ones when the rigidity of the slab fell to almost zero and there was no difference between the case of $\alpha=1.0$, $\beta=1.0$ and the case of $\alpha=0.78$, $\beta=0.1$. At that time, since the element rigidity of the yielded elements became zero, deformation took place in the analysis so as to generate discontinuous steps in the area of the yielded elements. This area of the yielded elements almost coincided with the peeled-off part observed at the time of experiment (dotted lines shown in Fig.9(b)) and the result of analysis corresponded to the deformed condition of the slab in the experiment.

Judging from the comparison of the result of analysis and that of experiment as described in the above, the behaviour almost coincided, thus it was proved that the behaviour of the slab when reloaded in the experiment could be traced by the finite element elasto-plastic method.

4.5 Estimation of the Punching Strength

As mentioned above, it was proved that the ultimate strength when reloaded was decided by the resisting moment due to yielding of the reinforcement and adequacy of the failure model in Fig.14 was confirmed. In other words, it was confirmed that in the corroded RC slab, the shearing fracture just under the loading plate and the maximum vertical force which was transmitted by way of the diagonal cracks contribute to its punching strength, and this vertical force balanced with the resisting moment in the cross section that was composed of the cover including the main reinforcement.

If the ultimate strength of the corroded RC slab is going to be estimated in accordance with this failure mechanism, it could be done by adding up these two components contributing the punching strength. The portion of contribution to the punching strength by the shearing fracture just under the loading plate could be calculated by assuming that it follows the 1st term of the formula (1). On the other hand, with regard to the vertical force that is transmitted by way of the diagonal cracks could be calculated by the finite element elasto-plastic analysis. The punching strength of the corroded RC slabs thus estimated was summarized in Table 4 and it was verified that they almost conformed with the punching strength obtained in the experiment. Therefore, this method as mentioned above could be effective to estimate the punching strength of the corroded RC slab.

Table 4 Ultimate Strength.

Case	First Term in eq.(1) A	Ultimate Strength in FEM Analysis B	A+B	Punching Strength of RC Slabs in Experiment
α= 1.00 β= 1.00	38.1 tonf	22.0 tonf	60.1 tonf	51.5, 56.5 tonf
α= 0.78 β= 0.10	38.1 tonf	19.0 tonf	57.1 tonf	

5. CONCLUSION

The result of this investigation has been summarized using the RC slab specimens for road bridge as the followings:

(1) As the result of the loading test conducted on RC slabs damaged with galvanostatic corrosion, it was verified that the reduction of their punching strength were occurred.
(2) The causes of this reduction of punching strength were supposed to be that the cracks due to expansion of corrosion products generated along the horizontal plane at the level of the main and distribution reinforcement reduced the effect of the dowel action and bring the change of the failure mechanism of the RC slabs.
(3) As the result of investigation made on the failure mechanism of the corroded RC slab, it was made clear that the shearing fracture just under the loading plate and the vertical force which was transmitted by way of the diagonal cracks contribute to its punching strength, and that this vertical force balances with the resisting moment in the cross section composed of the cover including the main reinforcement.
(4) As one of the methods to estimate the punching strength of the corroded RC slabs, it was shown that the portion of the shearing fracture which contributed the punching strength could be evaluated by the 1st term of the formula (1) and the vertical force which was transmitted by way of the diagonal cracks could be evaluated by the finite element elasto-plastic analysis.

In this study, it was shown that one of the damage factors influenced on the punching strength of corroded RC slabs was the horizontal cracked face generated caused by expansion of corrosion products. Thus, this generation of the horizontal cracked face was shown to be a turning point for discussing the mechanical behaviour of RC slabs damaged by corrosion of reinforcement on which the authors had reported in the literature[4]. For the actual structure, the prediction of growth of cracks due to corrosion products, the method of detecting cracks are considered to be important. And in order to evaluate the damaged structure, it will be necessary to conduct the investigation by the non-destructive testing method combined with the mechanical behaviour[17]~[19].

Finally, authors would like to express their sincere appreciation to the students in the Structure and Material Research Laboratory of the Department of the Civil Engineering of Kanazawa University, Dr. Ken-ichi Maeda and Mr.Takayuki Sakuta who offered us much co-operation.

References

[1] Page,C.L., Treadaway,K.W.J. and Bamforth,P.B.: Corrosion of Reinforcement in Concrete. Elsevier Applied Science, 1990.
[2] Kobayashi,K.: Mechanism of Deterioration of Concrete Structures by Corrosion of Reinforcement. The Civil Engineering Journal, Vol.25 No.10, pp.89-94, 1984. (in Japanese)
[3] Kobayashi,S.: Damage in Road Bridges. Concrete Journal, Vol.25, No.11, pp.53- 56, 1987. (in Japanese)
[4] Tachibana,Y., Kajikawa,Y. and Kawamura,M.: The Mechanical Behaviour of RC Beams Damaged by Corrosion of Reinforcement. Concrete Library International JSCE No.14. pp.177-188, 1990.
[5] Maeda,K., Tachibana,Y., Kajikawa,Y. and Tsunomoto,M.: The Mechanical Behaviour of RC Members Damaged by Corrosion of Reinforcement. Journal of Structural Engineering, Vol.35A, pp.1115-1128, 1989. (in Japanese)
[6] Wayers,R.E. and Cady,P.D.: Deterioration of Concrete Bridge Deck for Corrosion of Reinforcing Steel, Concrete International, Vol.9, No.1, pp.15-20, 1987.
[7] Maeda,Y. and Matsui,S.: Punching Shear Load Equation of Reinforced Concrete Slabs. Proceeding of JSCE, No.348/V-1, pp.133-141. 1984. (in Japanese)
[8] Sonoda,K. and Horikawa,T.: On Evaluation of Stresses under Wheel Loading for Road Bridge Deck Slabs. Proceeding of JSCE, No.273, pp.15-22, 1978. (in Japanese)
[9] Koyanagi,W.: On the Punching Strength of Concrete Slabs. Concrete Journal, Vol.19, No.8, pp.3-13, 1981. (in Japanese)
[10] Joint ACI-ASCE Committee 426: The Shear Strength of Reinforced Concrete Members-Slabs. Proc. of ASCE, Vol.100, No.ST8, pp.1543-1591, 1974.
[11] Kakuta,Y., Itoh,A. and Fujita,Y.: Experimental Study on Punching Strength of Reinforced Concrete Slabs. Proceeding of JSCE, No.229, pp.105-115, 1974. (in Japanese)
[12] Higai,T.: Experimental Study on Ultimate Strength of Reinforced Concrete Slabs. Year Report of Japan Highway, pp.140-149, 1975. (in Japanese)
[13] JSCE Concrete Library. No.61, pp.170-172, 1986. (in Japanese)
[14] Year Report of the Public Works Research Institute, p.196, 1989. (in Japanese)
[15] Aoyagi,Y. and Yamada,K.: Strength and Deformation Characteristics of Reinforced Concrete Shell Elements Subjected to In-plane Force. Proceeding of JSCE, No.331, pp.167-180, 1983. (in Japanese)
[16] Yamada,Y. and Yokouchi,Y.: Explanation of EPIC4. Baifukan, 1981. (in Japanese)
[17] Tsunomoto,M., Kajikawa,Y. and Kawamura,M.: Elasto-Plastic Analysis of Expansive Behaviour due to Corrosion of Reinforcement, Concrete Library International JSCE No.14, pp.189-199, 1990.
[18] Tachibana,Y., Maeda,K., Shigeishi,M. and Kajikawa,Y.: Study for the Use of Acoustic Emission on RC Slab Inspection Methods. Proceedings of the Japan Concrete Institute, 11-1, pp.337-342, 1989. (in Japanese)

[19] Tachibana,Y., Machida,F., Maeda,K. and Kajikawa,Y.: Failure Mechanism and Non-Destructive Inspection Method for RC slabs Damaged by Corrosion of Reinforcement. Proceeding of The Symposium on Non-Destructive Evaluation in Civil Engineering JSCE, pp.233-240, 1991. (in Japanese)